

See discussions, stats, and author profiles for this publication at: <https://www.researchgate.net/publication/274087748>

# Indirect-to-Direct Band Gap Crossover in Few-Layer MoTe<sub>2</sub>

ARTICLE in NANO LETTERS · MARCH 2015

Impact Factor: 13.59 · DOI: 10.1021/nl5045007 · Source: PubMed

CITATIONS

11

READS

107

7 AUTHORS, INCLUDING:



[Ignacio Gutierrez Lezama](#)

University of Geneva

16 PUBLICATIONS 318 CITATIONS

[SEE PROFILE](#)



[Ashish Arora](#)

University of Münster

13 PUBLICATIONS 54 CITATIONS

[SEE PROFILE](#)



[Celine Barreateau](#)

University of Geneva

17 PUBLICATIONS 283 CITATIONS

[SEE PROFILE](#)



[E. Giannini](#)

University of Geneva

119 PUBLICATIONS 1,168 CITATIONS

[SEE PROFILE](#)

# Indirect-to-Direct Band Gap Crossover in Few-Layer MoTe<sub>2</sub>

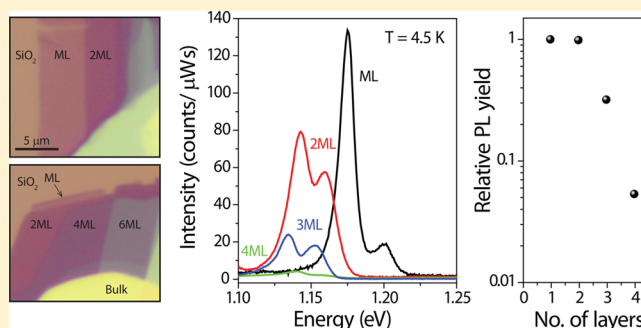
Ignacio Gutiérrez Lezama,<sup>\*,†,‡</sup> Ashish Arora,<sup>§</sup> Alberto Ubaldini,<sup>†</sup> Céline Barreteau,<sup>†</sup> Enrico Giannini,<sup>†</sup> Marek Potemski,<sup>§</sup> and Alberto F. Morpurgo<sup>\*,†,‡</sup>

<sup>†</sup>DPMC and <sup>‡</sup>GAP, Université de Genève, 24 quai Ernest Ansermet, CH-1211 Geneva, Switzerland

<sup>§</sup>Laboratoire National des Champs Magnétiques Intenses (LCNMI), CNRS, 25 rue des Martyrs B.P. 166, 38042 Grenoble, France

**ABSTRACT:** We study the evolution of the band gap structure in few-layer MoTe<sub>2</sub> crystals, by means of low-temperature microreflectance (MR) and temperature-dependent photoluminescence (PL) measurements. The analysis of the measurements indicate that in complete analogy with other semiconducting transition metal dichalcogenides (TMDs) the dominant PL emission peaks originate from direct transitions associated with recombination of excitons and trions. When we follow the evolution of the PL intensity as a function of layer thickness, however, we observe that MoTe<sub>2</sub> behaves differently from other semiconducting TMDs investigated earlier. Specifically, the exciton PL yield (integrated PL intensity) is identical for mono and bilayer, decreases slightly for trilayer, and it is significantly lower in the tetralayer. The analysis of this behavior and of all our experimental observations is fully consistent with mono and bilayer MoTe<sub>2</sub> being direct band gap semiconductors with tetralayer MoTe<sub>2</sub> being an indirect gap semiconductor and with trilayers having nearly identical direct and indirect gaps. This conclusion is different from the one reached for other recently investigated semiconducting transition metal dichalcogenides for which monolayers are found to be direct band gap semiconductors, and thicker layers have indirect band gaps that are significantly smaller (by hundreds of meV) than the direct gap. We discuss the relevance of our findings for experiments of fundamental interest and possible future device applications.

**KEYWORDS:** Molybdenum ditelluride, semiconducting transition metal dichalcogenides, 2D crystals, photoluminescence, reflectance, band gap crossover, exciton and trion



Thin layers of semiconducting transition metal dichalcogenides (TMDs) have received much attention due to their very interesting and rich optoelectronic properties,<sup>1–4</sup> which largely originate from the indirect-to-direct band gap crossover occurring when these materials are thinned down to a single monolayer (ML).<sup>5–11</sup> This crossover is not only responsible for a large enhancement of the photoluminescence (PL) quantum yield,<sup>5,7</sup> resulting in a strong increase in the intensity of emitted light but is also an essential condition for the observation of exciting phenomena resulting from valley-selective optical transitions,<sup>12–17</sup> such as the valley-Hall effect<sup>17,18</sup> and the possibility to control the spin and valley degrees of freedom.<sup>13–16</sup> First observed in MoS<sub>2</sub>,<sup>5,6</sup> the indirect-to-direct band gap crossover in monolayers has been found to be a common property of all the semiconducting TMDs investigated so far, including WS<sub>2</sub>,<sup>7</sup> WSe<sub>2</sub>,<sup>7</sup> and MoSe<sub>2</sub>.<sup>8,9</sup> The only difference between all these materials is of quantitative nature, that is, the magnitude of the band gap, of the exciton binding energy, spin–orbit splitting, and so forth (an interesting case is that of ReS<sub>2</sub>, which is a direct band gap semiconductor and remains so down to the monolayer<sup>19</sup>). The occurrence of such an identical behavior with only quantitative differences in the material parameters is being taken advantage of in the design of materials with engineered band structure, which can be

achieved by alloying transition metals and chalcogens with appropriate stoichiometry.<sup>20–23</sup>

Recently, we have started exploring (2H) MoTe<sub>2</sub>, one of the TMDs that has received limited attention so far,<sup>24–28</sup> focusing on the structure of the band gap in thick (>30 nm) exfoliated crystals.<sup>27</sup> We found that in these “bulk-like” crystals the difference between the indirect (0.88 eV) and direct band gap (1.02 eV) at room temperature is small, approximately only 0.15 eV (four-to-five times smaller than in all other TMDs investigated so far; in MoS<sub>2</sub>, for instance, this difference is approximately 0.7 eV<sup>29,30</sup>), and we suggested that because of this small difference the indirect-to-direct band gap crossover in MoTe<sub>2</sub> may occur already before reaching monolayer thickness. Here, we address this issue through a systematic study of the low-temperature PL and reflectivity in MoTe<sub>2</sub> crystals ranging from 1 to 5 MLs and find evidence supporting the hypothesis that the crossover from indirect to direct band gap does indeed occur before the monolayer limit. This result differs from that reported in a very recent study analogous to ours (see discussion at the end)<sup>28</sup> but that focused mainly on the analysis

**Received:** November 24, 2014

**Revised:** March 5, 2015

**Published:** March 24, 2015

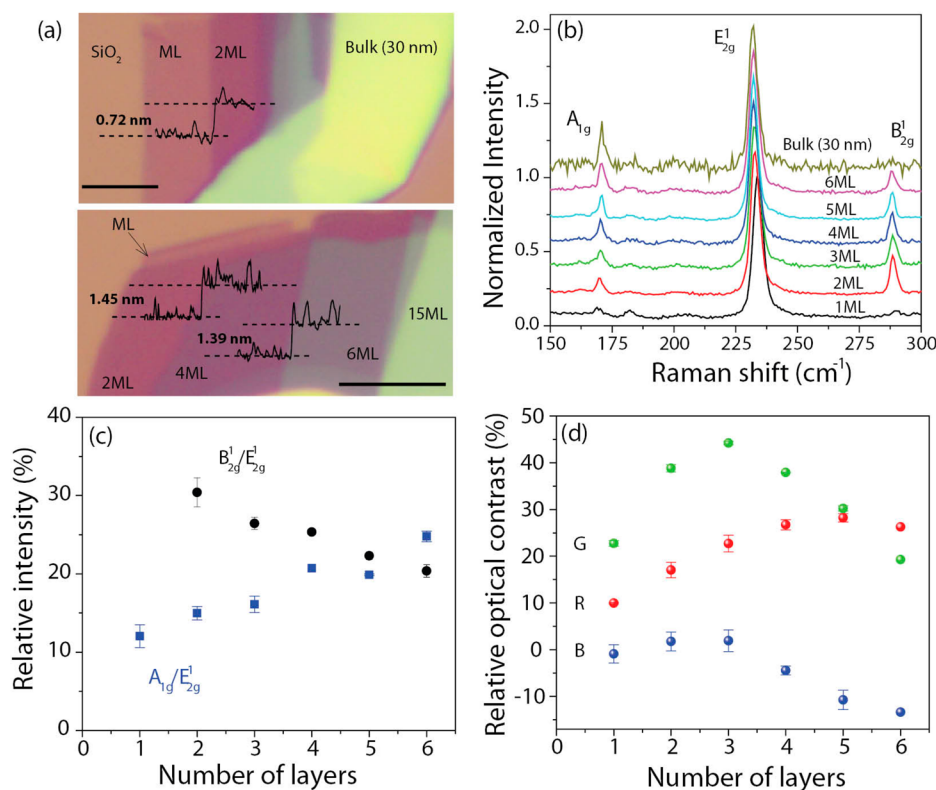


**Figure 1.** Characterization and identification of few-layer MoTe<sub>2</sub>. (a) Optical microscope images of multilayer MoTe<sub>2</sub> crystals and their corresponding AFM step height. The scale bars are 5  $\mu\text{m}$ . (b) Raman spectra of a bulk and ultrathin MoTe<sub>2</sub> crystals with thicknesses ranging from 1 to 6 ML. Curves offset for clarity. (c) Evolution of the relative Raman intensity of the A<sub>1g</sub> and B<sub>12g</sub> phonon modes with respect to the E<sub>12g</sub> mode. (d) Evolution of the relative optical contrast between the MoTe<sub>2</sub> crystals and the 290 nm SiO<sub>2</sub> substrate in the red (R), green (G), and blue (B) channels (note that a quantitative comparison requires care in performing all measurements with the same identically configured microscope and digital camera, because different microscopes and cameras can lead to somewhat different absolute intensity values).

of room-temperature measurements. We reach our conclusion by characterizing the direct excitonic transitions observed in PL and microreflectance (MR) measurements and by analyzing the evolution of the relative exciton PL yield (integrated PL intensity relative to the monolayer) with increasing thickness.

The atomically thin MoTe<sub>2</sub> layers studied here were exfoliated from two different sources (2Dsemiconductors Inc.<sup>31</sup> and Q-Mat<sup>32,33</sup>) with no significant difference in their optical properties. The exfoliated MoTe<sub>2</sub> layers were transferred onto Si substrates covered with a 290 nm SiO<sub>2</sub> layer and their thickness was determined through combined atomic force microscopy (AFM; Figure 1a) imaging, Raman spectroscopy (Figure 1b,c) and optical contrast measurements (Figure 1d). Specifically, the characterization of over 30 samples with thicknesses ranging from 1 to 6 MLs allowed us to identify two methods that can be used to determine the thickness unambiguously in a fast and noninvasive manner. These are the evolution of the relative intensity of Raman modes (Figure 1c) and the evolution of the difference in optical contrast with the underlying substrate (Figure 1d). Starting with the discussion of the Raman spectra, Figure 1b shows data for few-layer MoTe<sub>2</sub> crystals in which three distinctive peaks are observed,<sup>24,26</sup> the in-plane E<sub>12g</sub> mode ( $\sim 232\text{ cm}^{-1}$ ), the out-of-plane A<sub>1g</sub> mode ( $\sim 171\text{ cm}^{-1}$ ), and the bulk in-active B<sub>12g</sub> phonon mode ( $\sim 288\text{ cm}^{-1}$ , this latter peak, alternatively identified as the A<sub>21g</sub> in ref 26, is entirely absent in monolayers and easily enables their identification). The positions of the A<sub>1g</sub> and E<sub>12g</sub> peaks follow a systematic shift with decreasing the number of layers (Figure 1b).<sup>24,26</sup> Although in principle this

shift can be used to determine the layer thickness, in practice its magnitude is too small and susceptible to sample to sample variations to provide a reliable determination. Through a careful analysis, however, we succeeded in establishing that the relative peak intensities associated with the A<sub>1g</sub>, B<sub>12g</sub> (or A<sub>21g</sub>),<sup>26</sup> and E<sub>12g</sub> phonon modes do vary significantly and systematically upon varying the number of layers. As it is clear from Figure 1c, the relative changes in intensity are sufficiently large to provide a reliable thickness determination. Additionally, Figure 1d illustrates how the relative optical contrast  $C$  between the MoTe<sub>2</sub> crystals and the substrate ( $C = (I_{\text{sub}} - I_{\text{flake}})/I_{\text{sub}}$ , where  $I_{\text{sub}}$  and  $I_{\text{flake}}$  are the intensity of the substrate and of the crystal, measured with a digital camera under an optical microscope) also evolves systematically with layer thickness. Looking at this contrast, therefore, also provides an unambiguous thickness determination<sup>27</sup> (note that to perform this comparison correctly, care needs to be taken to use for all flakes an identically configured microscope with the same numerical aperture, light intensity, and digital camera).

We have performed temperature-dependent PL and low-temperature MR measurements on MoTe<sub>2</sub> crystals with thickness ranging from one to five layers. The PL measurements were performed using an Ar ion laser with an excitation wavelength of 488 nm and a spot size of  $\sim 2\text{ }\mu\text{m}$ . The PL emission from the sample was then dispersed using a 0.3 m focal length monochromator and detected with a liquid-nitrogen cooled InGaAs array detector. During the experiments, the laser power was varied between 0.5 and 128  $\mu\text{W}$ , resulting in a linear response of the PL intensity. In turn, the

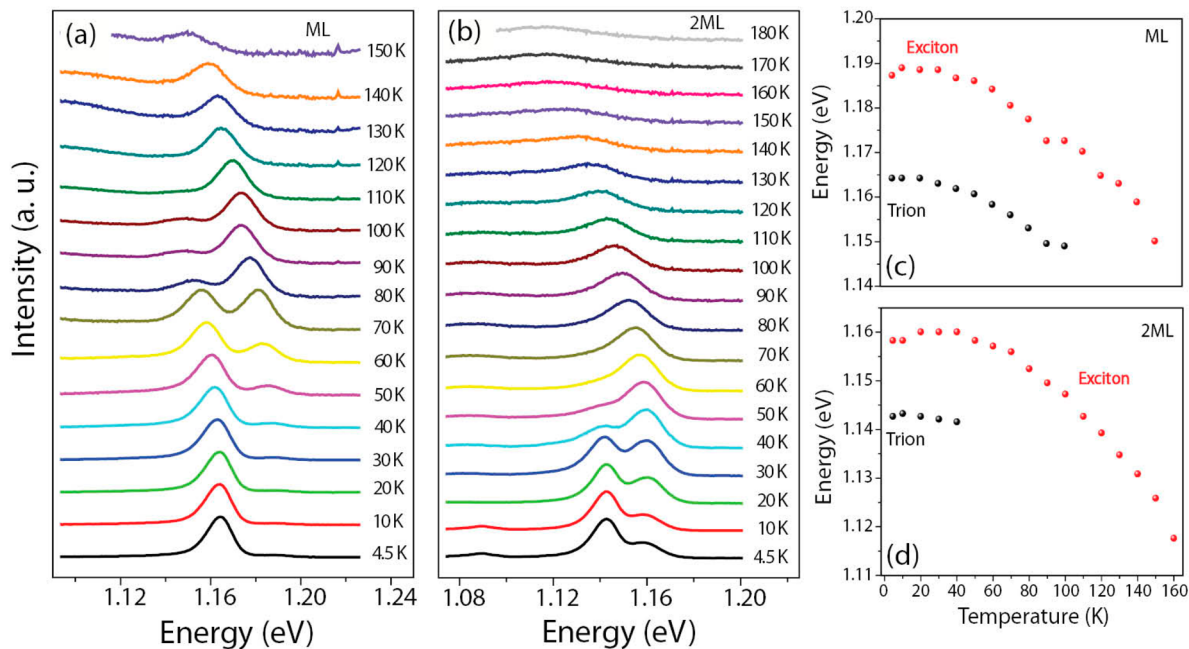


**Figure 2.** Normalized temperature-dependent PL spectra of mono (a) and bilayer (b) MoTe<sub>2</sub> measured with a 125 and 50  $\mu$ W laser power, respectively. The observed PL is by the A exciton in which at low temperature the exciton and trion contributions are resolved. The curves are offset for clarity. (c) Mono and (d) bilayer exciton and trion transition energies extracted from the spectra shown in (a,b). The difference between the two excitations is constant and corresponds to the trion binding energy, as discussed in the main text.

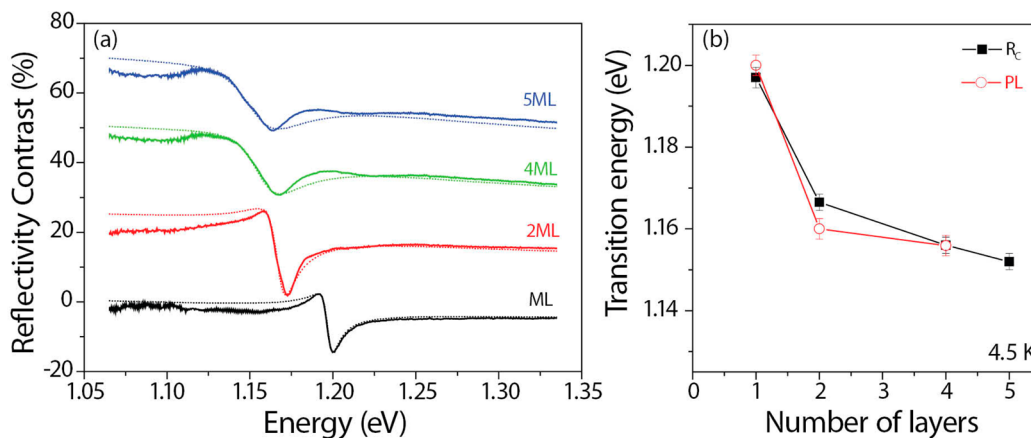


**Figure 3.** (a) Reflectivity contrast spectra of few-layer MoTe<sub>2</sub> measured at  $T = 4.5$  K. The spectra, which have been offset for clarity, show a dip corresponding to the A exciton transition, whose energy undergoes a blue shift with decreasing layer thickness. The dotted lines are the theoretical fits to extract the transition energies, as discussed in the main text. The position of the transition energy extracted from the reflectivity measurements (full squares) and from PL (open circles) are in very good agreement.

MR measurements were performed using collimated light from a 100 W tungsten halogen lamp focused through a pinhole of 150  $\mu$ m diameter, which was then collimated again before it was focused on the sample (spot size 3–4  $\mu$ m). The detection arrangement was similar to the one used during the PL measurements. During the measurements the samples were kept cold by direct contact with the coldfinger of a liquid-He continuous-flow cryostat, which allowed us to vary the sample temperature between 4 and 300 K.

As a first step, we identify the origin of spectral features observed in the PL and MR spectra of atomically thin MoTe<sub>2</sub> layers. The temperature dependence of the normalized PL spectra of mono and bilayer are shown in Figure 2a,b, respectively. The same general trend is observed in both cases. At low temperature (4.5 to 100 K) the PL line shape

consists of a split-peak that evolves into a single peak as the spectral weight of the low-energy peak is transferred to the high-energy one with increasing temperature (at the lowest temperatures, the high-energy peak in the monolayer is less pronounced and becomes more easily visible starting from 50 to 60 K). The split peak also undergoes a red shift with increasing temperature, leaving the energy difference between the two maxima constant (see Figure 2c,d). The above trends are all consistent with the expected temperature dependence of the PL emitted by 2D excitons (high-energy peak) and trions (low-energy peak), as it has been found previously in monolayer MoSe<sub>2</sub>.<sup>34</sup> These observations therefore establish the origin of the optical transitions that we observe in MoTe<sub>2</sub>. From the energy difference between the two peaks, we can also extract the trion binding energy<sup>34</sup> (see Figure 2c,d),



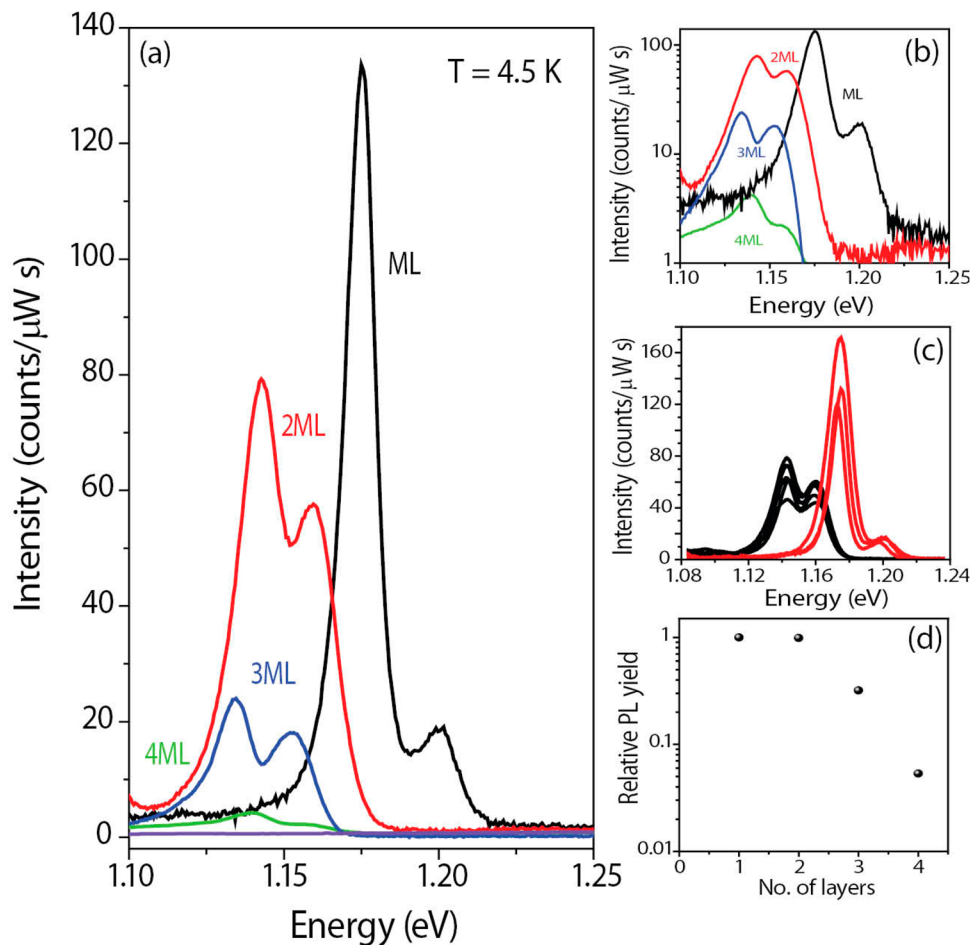


**Figure 4.** Photoluminescence spectra of few-layer  $\text{MoTe}_2$  measured at  $T = 4.5$  K and a laser power of  $128 \mu\text{W}$ , plotted in linear (a) and semilog scale (b). The two peaks observed in the spectra originate from the radiative recombination of trions (low-energy peaks) and excitons (high-energy peaks), whose transition energies undergo a blue shift with decreasing layer thickness. (c) The sample-to-sample reproducibility of the results, by showing PL spectra measured on several  $\text{MoTe}_2$  mono and bilayers. (d) The evolution of the relative exciton PL yield for  $\text{MoTe}_2$  layers of different thickness (from one to four layers).

corresponding to  $25 \pm 1$  and  $17 \pm 1$  meV for monolayers and bilayers, respectively. Because, as the temperature rises and electrons (or holes) escape their bound trion state due to thermal fluctuations, the lower binding energies found in bilayers, as compared to monolayers, are consistent with the disappearance of the trion peak at lower temperatures (see Figure 2a,b). The value found for the trion binding energies are comparable to those reported for other ultrathin semiconducting TMDs, such as monolayer  $\text{MoSe}_2$  (30 meV),<sup>34</sup> monolayer  $\text{MoS}_2$  (18 meV),<sup>35</sup> and bilayer  $\text{WSe}_2$  (30 meV),<sup>36</sup> demonstrating the consistency of our interpretation.

To confirm that the PL emission originating from excitons and trions is due to direct optical transitions, as expected, we have compared the PL spectra of few-layer  $\text{MoTe}_2$  crystals to the low-temperature MR spectra (Figure 3a), which on atomically thin layers are only sensitive to direct optical transitions.<sup>6,7</sup> Figure 3a shows the low-temperature reflectance spectra in terms of the reflectivity contrast  $R_C = (R_{C+S} - R_S)/(R_{C+S} + R_S)$ , where  $R_{C+S}$  and  $R_S$  are the reflectance measured on the crystal and on the substrate. We find that all the spectra in Figure 3a show a dip in reflectivity contrast at energies close to those of the exciton transition energies measured in layers of the same thickness (see Figures 2a,b and 4a; on the substrate used for MR measurements no trilayers were found, which is

why the corresponding spectrum is not present in Figure 3a). To compare quantitatively the position of the different features, we have extracted the precise value of the transition energy by fitting the  $R_C$  spectra using a standard multilayer transfer matrix method<sup>37,38</sup> in which the excitonic contribution to the dielectric function of the ultrathin  $\text{MoTe}_2$  crystals was assumed to be a Lorentzian. Although the fits do not reproduce the entire background in the  $R_C$  spectra, they do reproduce the transition region sufficiently reliably to enable the determination of the transition energies (see Figure 3a). The quantitative comparison between the transition energies extracted from the  $R_C$  spectra and the exciton transition energies measured in the PL spectra is shown in Figure 4a (the PL spectrum of the pentalayer is not shown because the signal is only slightly larger than the background emission coming from the Si substrate and cannot be disentangled from it). The good correspondence between PL and MR data (in all cases where the comparison could be made) is clear. It confirms that the observed transitions are direct and is consistent with what is expected from the so-called A-exciton, whose spectral weight is divided into an exciton and a trion contribution.<sup>34</sup>

Having identified the origin of the PL in few-layer  $\text{MoTe}_2$  as due to direct transitions associated with the A exciton, we analyze the evolution of the transition energy and PL intensity

with layer thickness. As shown in Figure 4a, the A exciton transition energy blue shifts with decreasing thickness, while the associated PL intensity increases (all the spectra were measured at the same laser power). Although these trends have been observed in the previously investigated thin-layer semiconducting TMDs,<sup>5,7,11</sup> the behavior of MoTe<sub>2</sub> is distinctively different. When passing from bi- to monolayer the increase of the maximum PL intensity is only a factor of 2–3 (see Figure 4a,b), an effect much smaller than that observed in other semiconducting TMDs.<sup>5,8</sup> To ensure that what we observe is not an artifact of a specific sample in which the monolayer PL is coincidentally quenched by some extrinsic mechanism, we have performed measurements on many different MoTe<sub>2</sub> bi- and monolayers and have found a very high reproducibility of our observations, as shown in Figure 4c. We emphasize that the observed behavior also demonstrates that the PL intensity is not affected by the unintentional presence of doping, which, as we have described in our previous study,<sup>27</sup> exhibits large random sample-to-sample fluctuations in concentration that do not correlate with the high reproducibility of the PL intensity.<sup>39</sup>

Rather than looking at the peak intensity, a more appropriate way to systematically compare the strength of the PL signal for layers of different thickness is to consider the relative exciton PL yield  $I/I_{\text{mono}}$ , where  $I$  is the integrated exciton PL intensity (trion plus exciton spectral weight) of each layer and  $I_{\text{mono}}$  is that of the monolayer. This quantity is plotted in Figure 4d for crystals ranging from 1 to 4 MLs. The data show that the relative exciton PL yield of mono- and bilayer coincide and that for trilayers it is only approximately 3 times smaller than for mono- and bilayers. Only for tetralayers the relative exciton PL yield is suppressed substantially (a factor of 30) with respect to 1 ML. At a quantitative level, the evolution of the relative exciton PL yield in MoTe<sub>2</sub>, therefore, is clearly different than in other semiconducting TMDs, where a suppression of 1–2 orders of magnitude is already observed when passing from mono- to bilayer.<sup>5,7,8</sup>

Another important difference between MoTe<sub>2</sub> and previously studied thin-layer semiconducting TMDs is the absence of a PL peak associated with indirect transitions (Figure 4a).<sup>5,7</sup> What is seen in other semiconducting TMDs is that monolayers, because of their direct-gap character, do not show a PL peak associated with indirect transitions at higher energy (because electron–hole pairs relax rapidly to the K-point in the Brillouin zone, form an exciton, and recombine undergoing a direct transition). In bilayers, however, the indirect gap is significantly smaller than the direct one, and a large number of electron–hole pairs can relax in k-space to form indirect excitons (i.e., excitons with electrons and holes having different momenta). Part of these excitons decay radiatively leading to a measurable PL, whose intensity is experimentally found to be smaller than that of the direct exciton transition (measured in the same bilayer) by at most a factor of 3–4.<sup>5,7</sup> It is clear from the data of Figure 4a that in our experiments, an indirect transition with the intensity expected based on the analogy with other semiconducting TMDs would be well above the background (at least for mono to trilayer<sup>5,7</sup>), and therefore it should be detected if present. However, in the case of MoTe<sub>2</sub> no transition is seen experimentally.

All these experimental observations point to a clear difference in the electronic structure of MoTe<sub>2</sub> multilayers as compared to that of multilayers of other semiconducting TMDs investigated earlier. Finding that the relative PL yield of the direct transitions in bilayer and trilayer coincide with (or is

comparable to) that of monolayer is not compatible with the presence of an indirect transition, at an energy much smaller than that of the direct one. We can therefore directly conclude that in MoTe<sub>2</sub>, bilayer and trilayer have an indirect transition whose energy is either larger than that of the direct one, that is, the systems are direct gap semiconductors, or only just smaller, that is, the systems are indirect gap semiconductors, with an indirect gap nearly coincident with the direct one (with a difference being at most few times  $kT$ , i.e., a few meV). In particular, finding the same PL yield for mono and bilayers suggests that both systems are direct gap semiconductors; the fact that the PL yield in trilayers is only three times smaller than in monolayers suggests that in trilayers the indirect gap is smaller than (but almost coincides with) the direct one.

This scenario also explains the absence of indirect transitions in the PL spectra. In mono and bilayer MoTe<sub>2</sub>, they are not observable because the smaller direct band gap favors relaxation and recombination of excitons at the K points (i.e., they are direct band gap semiconductors). In trilayers, because of the nearly degenerate gaps the direct excitons give a stronger PL signal that eclipses the one from indirect excitons (i.e., in trilayers the indirect transition is masked by the direct one, which is more intense and virtually at the same energy). In the case of the tetralayer, the PL signal is comparable to the background and hence the expected indirect transition is masked by the PL signal emitted by the substrate. Indeed, the substrate emits in between 1 and 1.13 eV, which is the energy range in which the indirect transition is expected (0.95–1.16 eV), as given by the inferred bulk indirect gap at 4 K ( $\approx 0.95$  eV)<sup>40</sup> and the energy of the direct transition in the tetralayer (1.16 eV; see Figures 3b and 4a). Although the above discussion certainly cannot account in detail for the precise intensities of the PL transitions in multilayers of different thicknesses, which depend on the corresponding radiative and nonradiative rates, we conclude that the scenario proposed here is consistent with all our experimental observations (and we cannot easily conceive alternative possibilities to account for all our findings).

Our conclusion is different from that of Ruppert et al.,<sup>28</sup> who recently reported experiments analogous to ours (but mainly focusing on room-temperature measurements), and inferred from their measurements that bilayer MoTe<sub>2</sub> is an indirect band gap semiconductor. This discrepancy is related to the fact that in thin MoTe<sub>2</sub> flakes the differences in the size of the indirect and direct gaps in layers of different thickness are comparable to and for several thicknesses probably smaller than  $kT$  at room temperature. Indeed for the bulk the difference between the direct and indirect gap is only 150 meV;<sup>27</sup> as the layers are thinned down the indirect gap becomes larger and the direct one stays approximately constant, decreasing considerably the difference between the two. The peaks present in our low-temperature PL spectra are sufficiently sharp to enable an unambiguous comparison of the transition energies observed in the PL and reflectivity spectra of thin flakes. On the contrary, the broad peaks present in the room-temperature PL spectra shown by Ruppert et al.<sup>28</sup> make the analysis more complex.

Specifically, a key difference between the observations of Ruppert et al.<sup>28</sup> and ours is the relation between the energy of the transitions observed in the PL and MR measurements. Ruppert et al.<sup>28</sup> observe that except for monolayers the PL signal is a broad signal that always peaks at an experimentally significantly lower energy than the MR signal (whereas in our case the two energies coincide, see Figure 3b). Because in very

thin layers an MR signal is only seen for direct transitions, they are forced to conclude that two transitions are actually present, and that the one at lower energy, manifesting itself in the PL signal and not in the MR measurements, must be an indirect transition (which implies that bi- and thicker layers are indirect gap semiconductors). In this scenario, however, it is difficult to understand why the direct transition inferred from MR measurements does not give any visible PL signal. As explicitly discussed in ref 28, the high temperature at which their measurements are carried out further complicates the interpretation by not allowing them to resolve if there are actually two peaks present in the PL spectra, calling for systematic low-temperature measurements. These low-temperature measurements are the focus of the work presented here and give experimental results that lead to the scenario explained above, providing evidence that both mono- and bilayers are direct band gap semiconductors.

We conclude that when the thickness of the material is reduced to a few atomic layers, the behavior of  $\text{MoTe}_2$  differs from that of previously studied semiconducting TMDs. This finding is interesting. Whereas previous studies appeared to establish the notion that all few-layer semiconducting TMDs have a qualitatively identical behavior, differing only for the precise values of the relevant energy scales, our results show that care needs to be taken. For fundamental physics, finding that  $\text{MoTe}_2$  bilayers have a high PL intensity can have implications for future experiments. For instance, recent theoretical calculations predict the closing of the band gap (at the K–K points) in bilayer semiconducting TMDs upon the application of a perpendicular electric field,<sup>41,42</sup> and in  $\text{MoTe}_2$  bilayers the enhanced PL could provide a particularly sensitive way to probe the evolution of the gap experimentally (e.g., in devices with ionic liquid gates that enable large perpendicular electric fields to be applied). In terms of potential for electronic applications, our results are also of interest. As it is common to all semiconducting TMDs investigated so far, a large PL combined with balanced (and sufficiently high) electron and hole mobility values (which for  $\text{MoTe}_2$  has already been reported in thicker exfoliated crystals<sup>27</sup>) are potentially useful for the realization of light-emitting devices. In this context, mono and bilayer  $\text{MoTe}_2$  are particularly interesting, because having excitons at much lower energies than other few layers TMDs they can enable the realization of devices operating in the far-infrared. Finally, we also note that the excitonic transitions in  $\text{MoTe}_2$  mono and bilayers are very close to the 1.3 eV band gap needed for maximum efficiency in single junction solar cells,<sup>3</sup> making these system worth investigating for photovoltaic applications.

## AUTHOR INFORMATION

### Corresponding Authors

\*E-mail: Ignacio.gutierrez@unige.ch (I.G.L.).

\*E-mail: alberto.morpurgo@unige.ch (A.F.M.).

### Present Address

(A.U.) Università degli Studi di Salerno, Istituto Superconduttori, Materiali innovativi e Dispositivi del Consiglio Nazionale delle Ricerche, Via Giovanni Paolo II, 132-84084 – Fisciano (SA), Italia.

### Author Contributions

I.G.L. prepared and identified the  $\text{MoTe}_2$  layers and did the optical measurements together with A.A. A.U., C.B., and E.G. grew and characterized the  $\text{MoTe}_2$  crystals used to produce

ultrathin crystalline layers. I.G.L., A.A., M.P., and A.F.M. analyzed and interpreted the data. I.G.L. did most of the manuscript writing with significant input from A.A., M.P., and A.F.M.. All authors discussed the results and commented the final manuscript.

### Notes

The authors declare no competing financial interest.

## ACKNOWLEDGMENTS

We gratefully acknowledge A. Ferreira for technical support, A. Kuzmenko for fruitful discussions, N. Ubrig for support with the Raman measurements and S. Ghosh for useful suggestions during the building of the microreflectance setup. Financial support from the Swiss National Science Foundation, the European Graphene Flagship, and the ERC-2012-AdG-320590-MOMB grant is also acknowledged.

## REFERENCES

- (1) Wang, Q. H.; Kalantar-Zadeh, K.; Kis, A.; Coleman, J. N.; Strano, M. S. Electronics and Optoelectronics of Two-Dimensional Transition Metal Dichalcogenides. *Nat. Nanotechnol.* **2012**, *7*, 699–712.
- (2) Chhowalla, M.; Shin, H. S.; Eda, G.; Li, L.-J.; Loh, K. P.; Zhang, H. The Chemistry of Two-Dimensional Layered Transition Metal Dichalcogenide Nanosheets. *Nat. Chem.* **2013**, *5*, 263–275.
- (3) Jariwala, D.; Sangwan, V. K.; Lauhon, L. J.; Marks, T. J.; Hersam, M. C. Emerging Device Applications for Two-Dimensional Transition Metal Dichalcogenides. *ACS Nano* **2014**, *11*, 1102–1120.
- (4) Baugher, B. W. H.; Churchill, H. O. H.; Yang, Y.; Jarillo-Herrero, P. Optoelectronic Devices Based on Electrically Tunable P-N Diodes in a Monolayer Dichalcogenide. *Nat. Nanotechnol.* **2014**, *9*, 1–6.
- (5) Mak, K. F.; Lee, C.; Hone, J.; Shan, J.; Heinz, T. F. Atomically Thin  $\text{MoS}_2$ : A New Direct-Gap Semiconductor. *Phys. Rev. Lett.* **2010**, *105*, 136805.
- (6) Splendiani, A.; Sun, L.; Zhang, Y.; Li, T.; Kim, J.; Chim, C.-Y.; Galli, G.; Wang, F. Emerging Photoluminescence in Monolayer  $\text{MoS}_2$ . *Nano Lett.* **2010**, *10*, 1271–1275.
- (7) Zhao, W.; Ghorannevis, Z.; Chu, L.; Toh, M. Evolution of Electronic Structure in Atomically Thin Sheets of  $\text{WS}_2$  and  $\text{WSe}_2$ . *ACS Nano* **2012**, *7*, 791–797.
- (8) Tongay, S.; Zhou, J.; Ataca, C.; Lo, K.; Matthews, T. Thermally Driven Crossover from Indirect toward Direct Bandgap in 2D Semiconductors:  $\text{MoSe}_2$  versus  $\text{MoS}_2$ . *Nano Lett.* **2012**, *12*, 5576–5580.
- (9) Zhang, Y.; Chang, T.-R.; Zhou, B.; Cui, Y.-T.; Yan, H.; Liu, Z.; Schmitt, F.; Lee, J.; Moore, R.; Chen, Y.; et al. Direct Observation of the Transition from Indirect to Direct Bandgap in Atomically Thin Epitaxial  $\text{MoSe}_2$ . *Nat. Nanotechnol.* **2014**, *9*, 6–10.
- (10) Jin, W.; Yeh, P.-C.; Zaki, N.; Zhang, D.; Sadowski, J. T.; Al-Mahboob, A.; van der Zande, A. M.; Chenet, D. a.; Dadap, J. I.; Herman, I. P.; et al. Direct Measurement of the Thickness-Dependent Electronic Band Structure of  $\text{MoS}_2$  Using Angle-Resolved Photoemission Spectroscopy. *Phys. Rev. Lett.* **2013**, *111*, 106801.
- (11) Zeng, H.; Liu, G.-B.; Dai, J.; Yan, Y.; Zhu, B.; He, R.; Xie, L.; Xu, S.; Chen, X.; Yao, W.; et al. Optical Signature of Symmetry Variations and Spin-Valley Coupling in Atomically Thin Tungsten Dichalcogenides. *Sci. Rep.* **2013**, *3*, 1608.
- (12) Cao, T.; Wang, G.; Han, W.; Ye, H.; Zhu, C.; Shi, J.; Niu, Q.; Tan, P.; Wang, E.; Liu, B.; et al. Valley-Selective Circular Dichroism of Monolayer Molybdenum Disulphide. *Nat. Commun.* **2012**, *3*, 887.
- (13) Mak, K. F.; He, K.; Shan, J.; Heinz, T. F. Control of Valley Polarization in Monolayer  $\text{MoS}_2$  by Optical Helicity. *Nat. Nanotechnol.* **2012**, *7*, 494–498.
- (14) Zeng, H.; Dai, J.; Yao, W.; Xiao, D.; Cui, X. Valley Polarization in  $\text{MoS}_2$  Monolayers by Optical Pumping. *Nat. Nanotechnol.* **2012**, *7*, 490–493.



- (15) Zhang, Y. J.; Oka, T.; Suzuki, R.; Ye, J. T.; Iwasa, Y. Electrically Switchable Chiral Light-Emitting Transistor. *Science* **2014**, *344*, 725–728.
- (16) Jones, A. M.; Yu, H.; Ghimire, N. J.; Wu, S.; Aivazian, G.; Ross, J. S.; Zhao, B.; Yan, J.; Mandrus, D. G.; Xiao, D.; et al. Optical Generation of Excitonic Valley Coherence in Monolayer WSe<sub>2</sub>. *Nat. Nanotechnol.* **2013**, *8*, 634–638.
- (17) Mak, K. F.; McGill, K. L.; Park, J.; McEuen, P. L. Valleytronics. The Valley Hall Effect in MoS<sub>2</sub> Transistors. *Science* **2014**, *344*, 1489–1492.
- (18) Xiao, D.; Liu, G.-B.; Feng, W.; Xu, X.; Yao, W. Coupled Spin and Valley Physics in Monolayers of MoS<sub>2</sub> and Other Group-VI Dichalcogenides. *Phys. Rev. Lett.* **2012**, *108*, 196802.
- (19) Tongay, S.; Sahin, H.; Ko, C.; Luce, A.; Fan, W.; Liu, K.; Zhou, J.; Huang, Y.-S.; Ho, C.-H.; Yan, J.; et al. Monolayer Behaviour in Bulk ReS<sub>2</sub> due to Electronic and Vibrational Decoupling. *Nat. Commun.* **2014**, *5*, 3252.
- (20) Komsa, H.-P.; Krasheninnikov, A. V. Two-Dimensional Transition Metal Dichalcogenide Alloys: Stability and Electronic Properties. *J. Phys. Chem. Lett.* **2012**, *3*, 3652–3656.
- (21) Chen, Y.; Xi, J.; Dumcenco, D. O.; Liu, Z.; Suenaga, K.; Wang, D.; Shuai, Z.; Huang, Y.-S.; Xie, L. Tunable Band Gap Photoluminescence from Atomically Thin Transition-Metal Dichalcogenide Alloys. *ACS Nano* **2013**, *7*, 4610–4616.
- (22) Mann, J.; Ma, Q.; Odenthal, P. M.; Isarraraz, M.; Le, D.; Preciado, E.; Barroso, D.; Yamaguchi, K.; von Son Palacio, G.; Nguyen, A.; et al. 2-Dimensional Transition Metal Dichalcogenides with Tunable Direct Band Gaps: MoS<sub>2</sub>(1-x)Se<sub>2x</sub> Monolayers. *Adv. Mater.* **2014**, *26*, 1399–1404.
- (23) Feng, Q.; Zhu, Y.; Hong, J.; Zhang, M.; Duan, W.; Mao, N.; Wu, J.; Xu, H.; Dong, F.; Lin, F.; et al. Growth of Large-Area 2D MoS<sub>2</sub>(1-x)Se<sub>2x</sub> Semiconductor Alloys. *Adv. Mater.* **2014**, *26*, 2648–2653.
- (24) Yamamoto, M.; Wang, S. T.; Ni, M.; Lin, Y.-F.; Li, S.-L.; Aikawa, S.; Jian, W.-B.; Ueno, K.; Wakabayashi, K.; Tsukagoshi, K. Strong Enhancement of Raman Scattering from a Bulk-Inactive Vibrational Mode in Few-Layer MoTe<sub>2</sub>. *ACS Nano* **2014**, *4*, 3895–3903.
- (25) Lin, Y.-F.; Xu, Y.; Wang, S.-T.; Li, S.-L.; Yamamoto, M.; Aparecido-Ferreira, A.; Li, W.; Sun, H.; Nakaharai, S.; Jian, W.-B.; et al. Ambipolar MoTe<sub>2</sub> Transistors and Their Applications in Logic Circuits. *Adv. Mater.* **2014**, *26*, 3263–3269.
- (26) Pradhan, N. R.; Rhodes, D.; Feng, S.; Xin, Y.; Moon, B.; Terrones, H.; Terrones, M.; Balicas, L. Field-Effect Transistors Based on Few-Layered  $\alpha$ -MoTe<sub>2</sub>. *ACS Nano* **2014**, *8*, 5911–5920.
- (27) Lezama, I. G.; Ubaldini, A.; Longobardi, M.; Giannini, E.; Renner, C.; Kuzmenko, A. B.; Morpurgo, A. F. Surface Transport and Band Gap Structure of Exfoliated 2H-MoTe<sub>2</sub> Crystals. *2D Mater.* **2014**, *1*, 021002.
- (28) Ruppert, C.; Aslan, O. B.; Heinz, T. F. Optical Properties and Band Gap of Single- and Few-Layer MoTe<sub>2</sub> Crystals. *Nano Lett.* **2014**, *14*, 6231–6236.
- (29) Kam, K.; Parkinson, B. Detailed Photocurrent Spectroscopy of the Semiconducting Group VI Transition Metal Dichalcogenides. *J. Phys. Chem.* **1982**, *86*, 463–467.
- (30) Cheiwchanchamnangij, T.; Lambrecht, W. R. L. Quasiparticle Band Structure Calculation of Monolayer, Bilayer, and Bulk MoS<sub>2</sub>. *Phys. Rev. B* **2012**, *85*, 205302.
- (31) 2D Semiconductors [www.2dsemiconductors.com](http://www.2dsemiconductors.com) (accessed May 2014).
- (32) Ubaldini, A.; Jacimovic, J.; Ubrig, N.; Giannini, E. Chloride-Driven Chemical Vapor Transport Method for Crystal Growth of Transition Metal Dichalcogenides. *Cryst. Growth Des.* **2013**, *13*, 4453–4459.
- (33) Q-Mat [www.q-mat.ch](http://www.q-mat.ch) (accessed April 2014).
- (34) Ross, J. S.; Wu, S.; Yu, H.; Ghimire, N. J.; Jones, A. M.; Aivazian, G.; Yan, J.; Mandrus, D. G.; Xiao, D.; Yao, W.; et al. Electrical Control of Neutral and Charged Excitons in a Monolayer Semiconductor. *Nat. Commun.* **2013**, *4*, 1474.
- (35) Mak, K. F.; He, K.; Lee, C.; Lee, G. H.; Hone, J.; Heinz, T. F.; Shan, J. Tightly Bound Trions in Monolayer MoS<sub>2</sub>. *Nat. Mater.* **2013**, *12*, 207–211.
- (36) Jones, A. M.; Yu, H.; Ross, J. S.; Klement, P.; Ghimire, N. J.; Yan, J.; Mandrus, D. G.; Yao, W.; Xu, X. Spin-layer Locking Effects in Optical Orientation of Exciton Spin in Bilayer WSe<sub>2</sub>. *Nat. Phys.* **2014**, *10*, 130–134.
- (37) Hecht, E. *Optics*, 3rd ed.; Addison-Wesley: Reading, MA, 1998.
- (38) Arora, A.; Mandal, A.; Chakrabarti, S.; Ghosh, S. Magneto-Optical Kerr Effect Spectroscopy Based Study of Landé G-Factor for Holes in GaAs/AlGaAs Single Quantum Wells under Low Magnetic Fields. *J. Appl. Phys.* **2013**, *113*, 213505.
- (39) Discussing the doping or carrier density dependence of the PL intensity is relevant, specifically in view of the comparison of our work with that of Ruppert et al.<sup>28</sup> In particular, we note that at room temperature the PL intensity depends strongly on the charge carrier density (see, for example, Newaz, A. K. M.; Prasai, D.; Ziegler, J. I.; Caudel, D.; Robinson, S.; Haglund, R. F., Jr.; Bolotin, K. I. Electrical Control of Optical Properties of Monolayer MoS<sub>2</sub>. *Solid State Commun.* **2013**, *155*, 49–52) whereas at lower temperature it does not (refs 34 and 35). Because most measurements shown by Ruppert et al.<sup>28</sup> are at room temperature, the effect of unintentional doping may be relevant in their case but does not affect our conclusions that are based on the measurements we performed at low temperature..
- (40) Lepetit, A. Propriétés Semiconductrices Du Diteleurure de Molybdène. *J. Phys. (Paris)* **1965**, *26*, 175–179.
- (41) Ramasubramanian, A.; Naveh, D.; Towe, E. Tunable Band Gaps in Bilayer Transition-Metal Dichalcogenides. *Phys. Rev. B* **2011**, *84*, 205325.
- (42) Zibouche, N.; Philipsen, P.; Kuc, A.; Heine, T. Transition-Metal Dichalcogenide Bilayers: Switching Materials for Spintronic and Valleytronic Applications. *Phys. Rev. B* **2014**, *90*, 125440.